UNIVERSITAT POLITÈCNICA DE CATALUNYA BARCELONATECH

UPCommons

Portal del coneixement obert de la UPC

http://upcommons.upc.edu/e-prints

Aquesta és una còpia de la versió *author's final draft* d'un article publicat a la revista [*Physics in Medicine and Biology*].

URL d'aquest document a UPCommons E-prints: http://hdl.handle.net/2117/87628

Paper publicar[1] ***/ Published paper*:**

Gom, Carles, Andreo, Pedro, and Sempau, Josep (2016)
Monte Carlo calculation of beam quality correction factors in proton beams using detailed simulation of ionization chambers. Physics in Medicine and Biology, 61. 6. 2389-2406.
Doi: 10.1088/0031-9155/61/6/2389

[1] Substituir per la citació bibliogràfica corresponent

Monte Carlo calculation of beam quality correction factors in proton beams using detailed simulation of ionization chambers

Carles Gomà[1], Pedro Andreo[2] and Josep Sempau[3]

[1] Department of Physics, Swiss Federal Institute of Technology Zurich, Zurich, Switzerland.

[2] Department of Medical Physics, Karolinska University Hospital, Stockholm, Sweden.

[3] Institut de Tècniques Energètiques, Universitat Politècnica de Catalunya, Barcelona, Spain.

E-mail: carlesgoma@student.ethz.ch

Abstract.

This work calculates beam quality correction factors (k_Q) in monoenergetic proton beams using detailed Monte Carlo simulation of ionization chambers. It uses the Monte Carlo code PENH and the electronic stopping powers resulting from the adoption of two different sets of mean excitation energy values for water and graphite: (i) the currently ICRU 37 and ICRU 49 recommended $I_{\rm w} = 75\,\rm eV$ and $I_{\rm g} = 78\,\rm eV$ and (ii) the recently proposed $I_{\rm w} = 78\,\rm eV$ and $I_{\rm g} = 81.1\,\rm eV$. Twelve different ionization chambers were studied. The k_Q factors calculated using the two different sets of I-values were found to agree with each other within 1.6% or better. k_Q factors calculated using current ICRU I-values were found to agree within 2.3% or better with the k_Q factors tabulated in IAEA TRS-398, and within 1% or better with experimental values published in the literature. k_Q factors calculated using the new I-values were also found to agree within 1.1% or better with the experimental values. This work concludes that perturbation correction factors in proton beams—currently assumed to be equal to unity—are in fact significantly different from unity for some of the ionization chambers studied.

1. Introduction

The reference dosimetry of clinical proton beams is described in IAEA TRS-398 (Andreo *et al* 2000). According to its formalism, the absorbed dose to water (D_w) at the reference depth in a proton beam of quality Q is given by

$$D_{\mathrm{w},Q} = M_Q N_{D,\mathrm{w},Q_0} k_{Q,Q_0} \tag{1}$$

where M_Q is the ionization chamber reading corrected for all quantities of influence (except for the beam quality), N_{D,w,Q_0} is the calibration coefficient of the ionization chamber in terms of absorbed dose to water in the reference beam quality Q_0 (typically ^{60}Co gamma radiation) and k_{Q,Q_0} is the beam quality correction factor of the chamber. k_{Q,Q_0} corrects for the different response of the ionization chamber between the user beam quality Q and the calibration beam quality Q_0 and it is defined as the ratio of the ionization chamber calibration coefficients at the beam qualities Q and Q_0

$$k_{Q,Q_0} = \frac{N_{D,\mathrm{w},Q}}{N_{D,\mathrm{w},Q_0}} = \frac{D_{\mathrm{w},Q}/M_Q}{D_{\mathrm{w},Q_0}/M_{Q_0}}. \tag{2}$$

Ideally, it should be determined experimentally in a Primary or Secondary Standards Dosimetry Laboratory. When experimental k_{Q,Q_0} factors are not available, as it is commonly the case for proton beams, they may also be calculated theoretically as (Andreo 1992)

$$k_{Q,Q_0} = \frac{s_{\mathrm{w,air},Q}\ p_Q}{s_{\mathrm{w,air},Q_0}\ p_{Q_0}} \frac{W_{\mathrm{air},Q}}{W_{\mathrm{air},Q_0}} \tag{3}$$

where $s_\mathrm{w,air}$ is the water/air stopping-power ratio, p is the perturbation correction factor of the ionization chamber and W_air is the mean energy needed to create an ion pair in air, at the beam qualities Q and Q_0.

Sempau *et al* (2004) introduced an alternative approach to the calculation of beam quality correction factors, based on the detailed Monte Carlo simulation of ionization chambers. The authors defined a single chamber-specific (and beam quality-dependent) factor, f, that establishes the proportionality between the absorbed dose to water at a point in the absence of the detector (D_w) and the average absorbed dose to air in the ionization chamber sensitive volume ($\bar{D}_\mathrm{air}$), i.e. $D_\mathrm{w} = \bar{D}_\mathrm{air}\, f$. With this approach beam quality correction factors are calculated as (Andreo *et al* 2013)

$$k_{Q,Q_0} = \frac{f_Q}{f_{Q_0}} \frac{W_{\mathrm{air},Q}}{W_{\mathrm{air},Q_0}} = \frac{(D_\mathrm{w}/\bar{D}_\mathrm{air})_Q}{(D_\mathrm{w}/\bar{D}_\mathrm{air})_{Q_0}} \frac{W_{\mathrm{air},Q}}{W_{\mathrm{air},Q_0}}. \tag{4}$$

Compared to equation (3), this calculation method has the advantage that it does not depend on a separate account of $s_\mathrm{w,air}$ and p, and it avoids the questionable assumption of independent perturbation contributions in the latter.

Due to a lack of experimental data—and Monte Carlo calculated data using equation (4)—at the time of publication, IAEA TRS-398 used equation (3) to calculate k_{Q,Q_0} factors for an extensive set of ionization chamber models. For the particular case of proton beams, ionization chamber-specific perturbation correction factors (p_Q) were assumed to be unity, with an overall standard uncertainty of the order of 1%‡. As a consequence of this approximation and the uncertainty of the $s_{\mathrm{w,air},Q}$ values from Medin and Andreo (1997), k_{Q,Q_0} factors for proton beams were estimated to have a rather large combined standard uncertainty ($u = 1.7\,\%$ for cylindrical ionization chambers; $u = 2.1\,\%$ for plane-parallel chambers), as compared to high-energy photon beams ($u = 1.0\,\%$). Such a large uncertainty could lead to a poor agreement in the reference dosimetry of different proton therapy centres using different reference ionization chambers.

Several attempts have been made so far to reduce this uncertainty. Some authors have determined experimentally k_{Q,Q_0} factors for a few cylindrical ionization chambers in a proton beam using water calorimetry (Vatnitsky *et al* 1996, Medin *et al* 2006, Medin 2010). However, the experimental k_{Q,Q_0} factors available in the literature are scarce. Other authors have used Monte Carlo simulation methods to calculate different quantities entering in equation (3), namely water/air stopping-power ratios (Gomà *et al* 2013) and chamber-specific perturbation correction factors (Palmans and Verhaegen 1998, Palmans *et al* 2001, Verhaegen and Palmans 2001, Palmans *et al* 2002, Palmans 2006, Palmans 2011).

However, no detailed Monte Carlo simulations of ionization chambers—in the way they have been done for high-energy photon (Wulff *et al* 2008, González-Castaño *et al* 2009, Muir and Rogers 2010, Muir *et al* 2012, Erazo and Lallena 2013) and electron beams (Sempau *et al* 2004, Zink and Wulff 2008, Zink and Wulff 2012, Muir and Rogers 2014, Erazo *et al* 2014)—have been done so far for proton beams. The reason for that is twofold. First, Monte Carlo codes typically used in radiation dosimetry of radiotherapy beams, such as EGSnrc (Kawrakow 2000a) and PENELOPE (Baró *et al* 1995, Sempau *et al* 1997, Salvat 2014), which have been proven to accurately simulate the transport of radiation (especially low-energy electrons) in ionization chamber geometries (Kawrakov 2000b, Seuntjens *et al* 2002, Sempau and Andreo 2006), do not include the transport of protons. Second, other Monte Carlo codes typically used in radiation therapy which do include proton transport—mainly GEANT4 (Agostinelli *et al* 2003), FLUKA (Ferrari *et al* 2005, Battistoni *et al* 2007) and MCNPX (Waters *et al* 2002)—have not yet been shown to achieve the level of accuracy needed for ionization chamber simulations (Poon *et al* 2005, Elles *et al* 2008, Klingebiel *et al* 2011).

Recently, Salvat (2013) has developed PENH, an extension of the PENELOPE code that includes the transport of protons based on their electromagnetic interactions in matter. Proton nuclear interactions have not been included. Sterpin *et al* (2013) introduced proton nuclear interactions for six isotopes (^{1}H, ^{12}C, ^{14}N, ^{16}O, ^{31}P, ^{40}Ca) in PENH. However, the simulation of ionization chambers requires more than these six isotopes. Although not dominant, the effect of proton nuclear interactions cannot be neglected in proton therapy. Whereas the contribution of charged particles heavier than protons to the absorbed dose to water might, on a first approximation, be considered

‡ In dealing with the expression of uncertainties, this work follows the recommendations of the GUM (JCGM 2008).

negligible (Paganetti 2002, Fippel and Soukup 2004, Gomà *et al* 2013), the contribution of secondary protons (i.e. protons originating from non-elastic nuclear interactions) cannot be disregarded, as they contribute roughly to 10% of the dose deposited by a proton beam in the clinical energy range (Paganetti 2002).

The aim of this work is to calculate beam quality correction factors in monoenergetic proton beams, based on a detailed Monte Carlo simulation of ionization chambers in proton and ^{60}Co gamma radiation beams—i.e. using equation (4). k_{Q,Q_0} factors were calculated for a wide range of plane-parallel ionization chambers and a limited set of cylindrical ionization chambers. Two different sets of mean excitation energy values for water (I_w) and graphite (I_g) were used: (i) the ICRU 37 (ICRU 1984) and ICRU 49 (ICRU 1993) values currently in use ($I_\mathrm{w} = 75\,\mathrm{eV}$ and $I_\mathrm{g} = 78\,\mathrm{eV}$); and (ii) the latest I-values for water ($I_\mathrm{w} = 78\,\mathrm{eV}$, Andreo *et al* 2013) and graphite ($I_\mathrm{g} = 81.1\,\mathrm{eV}$, Burns *et al* 2014), to be recommended in a forthcoming ICRU report on key data for ionizing radiation dosimetry. Two different W_air values for proton beams were also used accordingly (Andreo *et al* 2013). The feasibility of Monte Carlo calculation of beam quality correction factors in proton beams was assessed by comparing the results with experimental data and theoretical calculations.

2. Materials and methods

We used ^{60}Co gamma radiation as the reference beam quality Q_0 and monoenergetic proton beams of energies from 70 to 250 MeV as the user beam quality Q. Note that, when the reference beam quality is ^{60}Co, the subscript Q_0 in k_{Q,Q_0} is typically ommited.

This section describes: (i) the Monte Carlo codes used in this work, (ii) the reference conditions used and the geometry of the simulations, (iii) the radiation sources, (iv) the transport simulation parameters, (v) the geometry of the simulated ionization chambers, and (vi) the $W_{\mathrm{air},Q}$ values used.

2.1. Monte Carlo simulation codes

In this work we used PENH (Salvat 2013) for the calculation of beam quality correction factors for proton beams. PENH is a Fortran subroutine package, which is linked to PENELOPE (Salvat 2014), thus allowing for the simulation of coupled proton-electron-photon transport processes. As main program, we used a version of PENEASY (Sempau *et al* 2011) that includes PENH. As mentioned above, the only drawback of PENH is that it does not include proton nuclear interactions and, therefore, it does not include the transport of the secondary protons originating from non-elastic nuclear interactions.

As the influence of secondary protons cannot be disregarded, we also used GAMOS (Arce *et al* 2014)—a Monte Carlo simulation software framework based on the GEANT4 toolkit—to generate a realistic phase-space file in water, just in front of the ionization chamber (see below). More specifically, we used GAMOSv4.1.0, which runs on GEANTv4.9.6p02. We used the *QGSP_BIC_EMY* physics list (Cirrone *et al* 2009)—

which combines the electromagnetic standard physics (*G4EmStandardPhysics_option3*) for the electromagnetic processes and the binary cascade model for the hadronic inelastic processes—together with the following options: (i) *G4EmPenelopePhysics* for the electromagnetic processes of photons, electrons and positrons; and (ii) *G4UrbanMscModel96* for the multiple Coulomb scattering of electrons.

2.2. Reference conditions and geometry of the simulations

For the reference beam quality ^{60}Co we followed the reference conditions described in IAEA TRS-398. That is, we defined a $20 \times 20 \times 15\,\mathrm{cm}^3$ water phantom and we set the reference depth (z_{ref}) to 5 g cm^{-2}, the source-to-chamber distance to 100 cm and the field size at the reference depth to $10 \times 10\,\mathrm{cm}^2$. For proton beams we also followed the reference conditions for monoenergetic proton beams described in IAEA TRS-398, but we set the reference depth to 2 g cm^{-2}, instead of 3 g cm^{-2}, as discussed in Gomà *et al* (2014). To speed up the simulations of proton beams, we used a water phantom of $20 \times 20 \times 5\,\mathrm{cm}^3$, since proton backscatter can be considered negligible—see for instance Salvat (2013).

The absorbed dose to water at the reference depth was calculated as the average absorbed dose to water scored in a disc of 1 cm of radius and 250 μm of thickness centred at z_{ref}. This is a procedure introduced by Sempau *et al* (2004) that has become a common method to compute D_{w} in f_Q calculations, where the absorbed dose to water in a point is approximated by the average absorbed dose to water scored in a small volume. $\bar{D}_{\mathrm{air}}$ was calculated as the average absorbed dose to air in the ionization chamber sensitive volume. For both ^{60}Co and proton beams the ionization chambers were positioned as described in IAEA TRS-398, i.e. the reference point of the chamber was positioned on the central axis of the beam at the reference depth. For cylindrical chambers the reference point is the centre of the cavity volume; for plane-parallel chambers it is on the inner surface of the entrance window at its centre. Some authors have questioned the IAEA TRS-398 recommendation of positioning the reference point of cylindrical chambers at the reference depth in monoenergetic proton beams (Palmans *et al* 2001, Palmans 2006, Gomà *et al* 2014, Gomà *et al* 2015). This point will not be addressed in this work. Herein we focus on the calculation of k_Q factors for plane-parallel chambers, which are not affected by this debate. We also simulated a limited set of cylindrical chambers, in order to validate our simulations with published experimental data.

2.3. Radiation sources

As ^{60}Co beam source we simulated a photon point source located 100 cm away from z_{ref} (i.e. 95 cm away from the water phantom surface), shaping a $10 \times 10\,\mathrm{cm}^2$ field at z_{ref}. The energy of the photons emerging from the source was sampled from the spectrum of the *Bureau International des Poids et Mesures* (BIPM) ^{60}Co-source calculated by Burns (2003). As this spectrum had been scored at a distance of 90 cm from the source,

Table 1: Equivalence between proton energy and range in water for different I_w-values. All range values (R_{CSDA}, R_{p} and R_{res}) are expressed in g cm^{-2}.

	$I_w = 75\,\mathrm{eV}$					$I_w = 78\,\mathrm{eV}$				
E (MeV)	70	100	150	200	250	70	100	150	200	250
R_{CSDA}	4.08	7.72	15.77	25.96	37.94	4.10	7.76	15.86	26.09	38.01
R_{p}	4.15	7.85	16.03	26.37	38.52	4.18	7.89	16.12	26.51	38.72
$R_{\mathrm{res}}\,(z_{\mathrm{ref}} = 2\,\mathrm{g\,cm^{-2}})$	2.15	5.85	14.03	24.37	36.52	2.18	5.89	14.12	24.51	36.72

we transported the photons through 90 cm of vacuum and 5 cm of air before reaching the water phantom.

As proton source we used a phase-space file (PSF) generated with GAMOS. We simulated a planar $10\times10\,\mathrm{cm}^2$ proton beam impinging on the surface of a water phantom. The incident protons were monoenergetic, monodirectional and perpendicular to the water phantom surface. We scored a PSF at the depth of 15 mm in water, including only those particles that PENH can transport, i.e. protons, electrons, positrons and photons. PSFs were generated for five different proton energies (70, 100, 150, 200 and 250 MeV) and they were subsequently used as input PSF sources in PENH. Table 1 shows the equivalence between the initial energy of the proton beam and the range in water for different I_w-values. R_{CSDA} is the continuous slowing down approximation range; R_{p} is the practical range, which is defined as the depth beyond the Bragg peak at which the absorbed dose falls to 10% of its maximum value (Andreo *et al* 2000); and R_{res} is the residual range, which is defined as the practical range minus the measurement depth (Andreo *et al* 2000) and in table 1 is given for a reference depth of $z_{\mathrm{ref}} = 2\,\mathrm{g\,cm^{-2}}$.

It is important to point out that, in the calculation of the beam quality correction factors, we assumed that the contribution to D_w from secondary protons and heavier charged particles generated in the vicinity of the reference point of measurement is comparable to the contribution to $\bar{D}_{\mathrm{air}}$ from secondary protons and heavier charged particles generated in the ionization chamber materials. Thus, this work assumes that these two contributions cancel out in the numerator of equation (4) and have therefore a negligible effect on the calculated k_Q values. This assumption is, of course, an additional source of uncertainty in the final k_Q factors.

2.4. Transport simulation parameters

2.4.1. GAMOS. In GAMOS we set the production cuts for photons, electrons and positrons to 2.5 μm, the absorption energies of photons to $E_{\mathrm{abs}}(\gamma) = 1\,\mathrm{keV}$, electrons and positrons to $E_{\mathrm{abs}}(e^-) = E_{\mathrm{abs}}(e^+) = 200\,\mathrm{keV}$ and protons to $E_{\mathrm{abs}}(p) = 1\,\mathrm{MeV}$. We limited the maximum step size of charged particles, so that they underwent at least 20 condensed simulation steps before reaching the PSF scoring plane.

2.4.2. PENH. The transport simulation parameters in PENH are the same as in PENELOPE and they are described in detail in Salvat (2014).

In this work all the simulations had the same structure: a scoring volume, a detailed simulation region (around the scoring volume) and a mixed (class II) (Berger 1963) simulation region (surrounding these two). The scoring volume was either the small disc of water, assumed to be good representative of a point, or the ionization chamber sensitive volume. The detailed and mixed simulation volumes were defined arbitrarily, but conservatively, as follows. We transported all electrons with energy higher than 200 keV, as these electrons have a radiation yield in water larger than 0.1%. Where the probability for a 200 keV electron of reaching the scoring volume was negligible, we set the absorption energy for electrons to $E_{\mathrm{abs}}(e^-) = 200\,\mathrm{keV}$; where it was non-negligible, we set it to $E_{\mathrm{abs}}(e^-) = 1\,\mathrm{keV}$. In water, for instance, we defined this probability based on the R_{CSDA} in water of a 200 keV electron, multiplied by a factor of 1.2—to account for the possibility that an electon may travel a distance beyond its R_{CSDA} due to energy-loss straggling (Sempau and Andreo 2006). In ionization chamber geometries the influence of the different materials was taken into account. Finally, we defined the detailed and mixed simulation volumes as the regions with $E_{\mathrm{abs}}(e^-) = 1\,\mathrm{keV}$ and $E_{\mathrm{abs}}(e^-) = 200\,\mathrm{keV}$, respectively.

Absorption energies for photons and protons were set to $E_{\mathrm{abs}}(\gamma) = 1\,\mathrm{keV}$ and $E_{\mathrm{abs}}(p) = 1\,\mathrm{MeV}$, respectively, for all regions. In the scoring volume and the detailed simulation region we used detailed simulation (i.e. we simulated every single interaction). Absorption energies for electrons and positrons were set to $E_{\mathrm{abs}}(e^-) = E_{\mathrm{abs}}(e^+) = 1\,\mathrm{keV}$ and all the transport simulation parameters (C_1, C_2, W_{cc}, and W_{cr}) for all charged particles were set to zero. In the mixed simulation region the absorption energy for electrons and positrons was 200 keV. For all charged particles we used $W_{\mathrm{cc}} = 10\,\mathrm{keV}$ and $W_{\mathrm{cr}} = 1\,\mathrm{keV}$ and we increased gradually C_1 and C_2 from 0.05 (everywhere in the mixed simulation region within a distance less than or equal to 5 mm from the scoring volume) to 0.1 (elsewhere). In the mixed simulation region we also set DSMAX in such a way that each charged particle underwent at least 20 artificial interactions—each one condensing the effect of many soft interactions—in each body.

To reduce the statistical uncertainty, we applied the variance reduction technique of particle splitting to all the particles arriving at the scoring volume, with a splitting factor of 10. We implemented particle splitting in such a way that split particles could not be split again.

Finally, all proton, electron and positron electronic stopping powers in the material data files were evaluated using the two sets of I_{w}- and I_{g}-values.

2.5. Ionization chambers

As mentioned above, this work focuses on the simulation of plane-parallel ionization chambers. We simulated accurately the geometry of nine different chambers: the Exradin A10, A11 and A11TW (Standard Imaging, Middleton WI, USA); the IBA

Table 2: Dimensions and material composition of the plane-parallel ionization chambers simulated in this work.

Ionization chamber	Entrance window thickness	Electrode spacing	Collecting electrode thickness	Sensitive volume radius	Guard ring width
Exradin					
A10	0.99 mm PMMA 0.10 mm air 25 μm kapton	2.01 mm	0.38 mm C552	2.85 mm	4.1 mm
A11	0.99 mm C552	2.01 mm	0.51 mm C552	9.93 mm	4.4 mm
A11TW	0.99 mm PMMA 0.10 mm air 25 μm kapton	3 mm	0.51 mm C552	9.93 mm	2.8–4.4 mm
IBA					
NACP-02	0.1 mm mylar 0.5 mm graphite ($\rho_{\mathrm{g}} = 1.82\,\mathrm{g\,cm^{-3}}$)	2 mm	50 μm graphite ($\rho_{\mathrm{g}} = 0.93\,\mathrm{g\,cm^{-3}}$) 0.25 mm rexolite	5 mm	3.25 mm
PPC-05	1 mm C552	0.6 mm	0.1 mm graphite ($\rho_{\mathrm{g}} = 1.7\,\mathrm{g\,cm^{-3}}$) 0.5 mm PEEK	4.95 mm	3.95 mm
PPC-40	0.9 mm PMMA 0.1 mm graphite ($\rho_{\mathrm{g}} = 0.93\,\mathrm{g\,cm^{-3}}$)	2 mm	0.1 mm graphite ($\rho_{\mathrm{g}} = 0.93\,\mathrm{g\,cm^{-3}}$)	8 mm	4.0 mm
PTW					
Advanced Markus	0.87 mm PMMA 0.4 mm air 30 μm polyethylene	1 mm	20 μm graphite ($\rho_{\mathrm{g}} = 0.82\,\mathrm{g\,cm^{-3}}$)	2.5 mm	2 mm
Markus	0.87 mm PMMA 0.4 mm air 30 μm polyethylene	2 mm	20 μm graphite ($\rho_{\mathrm{g}} = 0.82\,\mathrm{g\,cm^{-3}}$)	2.65 mm	0.25–0.35 mm
Roos	1.1 mm PMMA 20 μm graphite ($\rho_{\mathrm{g}} = 0.82\,\mathrm{g\,cm^{-3}}$)	2 mm	20 μm graphite ($\rho_{\mathrm{g}} = 0.82\,\mathrm{g\,cm^{-3}}$)	7.5 mm	4 mm

NACP-02, PPC-05 and PPC-40 (IBA Dosimetry GmbH, Schwarzenbruck, Germany); and the PTW Advanced Markus (Type 34045), Markus (Type 23343) and Roos (Type 34001) (PTW, Freiburg, Germany). For the Exradin and IBA plane-parallel chambers very detailed descriptions of the geometry and materials of the chambers were provided by the manufacturers. For the Exradin chambers geometry files were built from blueprints; for the IBA chambers we adapted the geometry files prepared by Sempau *et al* (2004). For the PTW chambers a less detailed description of the geometry and partial information of the materials of the chambers were also provided by the manufacturer. It is well-known that small variations in the dimensions and material composition of the detection volume and surrounding bodies (entrance window, collecting electrode, guard ring, etc.) have a significant effect on $\bar{D}_{\mathrm{air}}$. Table 2 summarizes the dimensions and material composition of the plane-parallel ionization chambers simulated in this work.

In addition to plane-parallel chambers, we also simulated three different models of cylindrical chambers: IBA FC65-G, IBA FC65-P and NE 2571. As mentioned above, we simulated this limited set of cylindrical chambers in order to validate our calculations with the few experimental data available in the literature (Palmans *et al* 2001, Palmans *et al* 2002, Medin *et al* 2006, Medin 2010, Gomà *et al* 2015). The geometry and materials of these chambers were taken from manufacturer information (drawings and technical specifications) available online. For the NE 2571 we simulated the geometry using the description and materials of NE (1984) and additional information taken from Aird and Farmer (1972) and Wulff *et al* (2008). Based on NE (1984), we assumed the insulator material to be polychlorotrifluoroethylene (PCTFE), instead of the polytetrafluoroethylene (PTFE) assumed by other authors (e.g. Wulff *et al* 2008, Erazo and Lallena 2013). Also, as the NE 2571 is not waterproof, we simulated a 0.5 mm PMMA sleeve around the chamber.

2.6. W_{air} value for proton beams

As pointed out by Andreo *et al* (2013)—where new I_{w}- and I_{g}-values were presented along with their impact on air kerma and absorbed dose to water standards—for proton beam dosimetry a change in I-values may also require a change in $W_{\mathrm{air},Q}$. In this work, in order to calculate beam quality correction factors in proton beams using equation (4), we are interested in the ratio between $W_{\mathrm{air},Q}$ and W_{air,Q_0}. When using ICRU I-values, we used the currently recommended W_{air} values ($W_{\mathrm{air},Q_0} = 33.97\,\mathrm{eV}$, $W_{\mathrm{air},Q} = 34.23\,\mathrm{eV}$) (Andreo *et al* 2000, ICRU 2007), so that $W_{\mathrm{air},Q}/W_{\mathrm{air},Q_0} = 1.008(4)$. According to Andreo *et al* (2013), the adoption of $I_{\mathrm{w}} = 78\,\mathrm{eV}$ and $I_{\mathrm{g}} = 81.1\,\mathrm{eV}$ should be accompanied with an increase in $W_{\mathrm{air},Q}$ of about 0.6% (i.e. $W_{\mathrm{air},Q} = 34.44\,\mathrm{eV}$), under the assumption of no changes in p_Q, while W_{air,Q_0} remains unchanged. Thus, when using these new I-values, we used $W_{\mathrm{air},Q}/W_{\mathrm{air},Q_0} = 1.014(4)$.

Table 3: Monte Carlo calculated f_{Q_0} factors (i.e. for ^{60}Co gamma radiation) for different plane-parallel ionization chambers and comparison with values in the literature. The values within parenthesis correspond to one standard uncertainty in the last digits.

Ionization chamber	This work $I_w = 78$ eV $I_g = 81.1$ eV	This work $I_w = 75$ eV $I_g = 78$ eV	Panettieri *et al* (2008)	Muir *et al* (2012)	Zink & Wulff (2012)	Erazo *et al* (2014)
Exradin						
A10	1.1225(20)	1.1249(20)		1.0951(5)		1.1088(26)
A11	1.1071(15)	1.1087(15)		1.1158(5)		1.1124(16)
A11TW	1.0979(14)	1.1016(14)				1.1055(16)
IBA						
NACP-02	1.1523(15)	1.1536(15)	1.1578(7)	1.1562(4)	1.1616(5)	1.1509(18)
PPC-05	1.1374(18)	1.1381(18)	1.1410(10)	1.1475(5)		
PPC-40	1.1403(12)	1.1468(12)	1.1455(7)	1.1440(5)		
PTW						
Adv. Markus	1.1470(23)	1.1464(23)		1.1446(5)	1.1478(6)	
Markus	1.1434(18)	1.1456(18)		1.1416(4)	1.1467(7)	
Roos	1.1406(12)	1.1459(12)		1.1485(5)	1.1509(5)	

Table 4: Monte Carlo calculated f_{Q_0} factors (i.e. for ^{60}Co gamma radiation) for cylindrical ionization chambers and comparison with values in the literature. The values within parenthesis correspond to one standard uncertainty in the last digit.

	$I_w = 75$ eV; $I_g = 78$ eV			$I_w = 78$ eV; $I_g = 81.1$ eV	
Ionization chamber	This work	Muir & Rogers (2010)	Andreo *et al* (2013)	This work	Andreo *et al* (2013)
IBA FC65-G	1.1123(9)	1.1134(5)		1.1050(9)	
IBA FC65-P	1.1169(9)	1.1134(5)		1.1145(9)	
NE 2571	1.1111(9)	1.1124(4)	1.114(1)	1.1039(9)	1.110(1)

3. Results and discussion

3.1. Reference beam quality

Table 3 and table 4 show the Monte Carlo calculated f_{Q_0} factors (i.e. for ^{60}Co gamma radiation) for the different plane-parallel and cylindrical ionization chambers studied in this work. We calculated the f_{Q_0} factors using the electronic stopping powers resulting from the adoption of two different sets of I-values for water and graphite: ICRU I-values ($I_w = 75$ eV; $I_g = 78$ eV) and new I-values proposed by Andreo *et al* (2013) and Burns *et al* (2014) ($I_\mathrm{w} = 78$ eV; $I_\mathrm{g} = 81.1$ eV).

Table 3 also shows other f_{Q_0} factors published in the literature for the same plane-parallel ionization chambers and calculated using ICRU I-values. Panettieri *et al* (2008) calculated the f_{Q_0} factor for the three IBA plane-parallel chambers studied in this work with PENELOPE-2006. The authors used three different ^{60}Co sources (a monoenergetic beam, a photon spectrum and a phase-space file). The values shown in table 3 are the f_{Q_0} factors corresponding to the weighted mean of the values obtained with the three different ^{60}Co sources. Muir *et al* (2012) calculated k_Q factors in megavoltage photon beams for most of the ionization chambers studied in this work with EGSnrc. Although the explicit f_{Q_0} factors were not reported in their work, the values in table 3 were provided by the authors in a private communication. For the NACP-02 f_{Q_0} factor table 3 shows the value corresponding to the geometry studied in this work (0.6 mm-thick entrance window, $\rho_\mathrm{g} = 1.82\,\mathrm{g\,cm^{-3}}$), also provided by the authors. Zink and Wulff (2012) calculated the perturbation correction factors p_{Q_0} for the NACP-02 and the three PTW chambers studied in this work with EGSnrc. The values shown in table 3 are the product of the reported p_{Q_0} factors and the IAEA TRS-398 water/air stopping power ratio for ^{60}Co ($s_{\mathrm{w,air},Q_0} = 1.133$). The uncertainty values shown in table 3 correspond to the uncertainty estimates given by these authors for the p_{Q_0} factors, i.e. they do not take the uncertainty of $s_{\mathrm{w,air},Q_0}$ into account. Again, for the NACP-02 f_{Q_0} factor we took the value corresponding to the geometry studied in this work. Finally, Erazo *et al* (2014) calculated k_{Q,Q_0} factors in electron beams for the NACP-02 and the three Exradin ionization chambers studied in this work with PENELOPE-2011. Although the explicit f_{Q_0} factors were not reported in their work, the values in table 3 were also provided by the authors in a private communication.

Table 4 also shows f_{Q_0} factors for cylindrical chambers published in the literature. Muir and Rogers (2010) calculated k_Q factors in megavoltage photon beams for the three cylindrical chambers studied in this work with EGSnrc and using ICRU I-values. Although the explicit f_{Q_0} factors were not reported in their work, the values in table 4 were provided by the authors in a private communication. Andreo *et al* (2013) calculated the f_{Q_0} factor of the NE 2571 for the same two sets of I-values studied in this work, also with EGSnrc.

For the plane-parallel ionization chambers studied in this work we found that the adoption of new I-values leads to a decrease in f_{Q_0} of around 0.2%, ranging from no changes (PTW Adv. Markus) to a decrease of about 0.6% (IBA PPC-40). It should be noticed that the estimate of Andreo *et al* (2013) for the decrease in $s_{\mathrm{w,air},Q_0}$, resulting from the adoption of new I-values, was 0.6%. Hence, the new I-values cause an increase in the perturbation correction factors for ^{60}Co estimated to be negligible for the IBA PPC-40 chamber and up to 0.6% for the PTW Adv. Markus, where the changes in $s_{\mathrm{w,air},Q_0}$ and p_{Q_0} practically cancel each other.

For cylindrical chambers the adoption of new I-values results in a decrease in f_{Q_0} of 0.2% for the IBA FC65-P and of about 0.7% for the graphite-walled chambers (IBA FC65-G and NE 2571). Thus, for graphite-walled cylindrical chambers the new I-values result in negligible changes in p_{Q_0}, which is consistent with the 0.2% increase estimated by Andreo *et al* (2013) for the NE 2571.

The vast majority of f_{Q_0} factors calculated in this work agree within 0.5% with the values published in the literature and calculated using the same I-values. These differences are consistent with the use of different Monte Carlo codes. In what follows we limit the discussion of the results to those differences larger than 0.5%.

For the Exradin A10 our f_{Q_0} factor differs by 1.5% and 2.7% from the values of Erazo *et al* (2014) and Muir *et al* (2012), respectively. Such large differences are only observed with this ionization chamber model. In addition to the Monte Carlo code (or its version) and the ^{60}Co spectrum used, there are two important differences between our simulations and those by these authors: (i) for the description of the geometry we used an updated version of the A10 blueprints provided by the manufacturer, fixing a 'bug' in the vicinity of the chamber sensitive volume; and (ii) the transport simulation parameters used in the chamber sensitive volume and surrounding bodies were rather different. Whereas our work used detailed simulation (i.e. all collisions were simulated), these authors used a mixed simulation scheme. The smaller the air cavity, the larger the influence of transport simulation parameters. This explains the larger effect on the A10 chamber, which has a small sensitive volume.

The f_{Q_0} factor of the NACP-02 chamber agrees within 0.2%, 0.2% and 0.4% with the values of Muir *et al* (2012), Erazo *et al* (2014) and Panettieri *et al* (2008), respectively, but it differs by 0.7% from the value of Zink and Wulff (2012). This discrepancy could be explained in terms of the different material composition of the collecting electrode used by Zink and Wulff (2012), which may affect f_{Q_0} by up to 0.5% (Muir *et al* 2012).

For the IBA PPC-05 our f_{Q_0} factor agrees within 0.3% with the value of Panettieri *et al* (2008), but it differs by 0.8% from the value of Muir *et al* (2012). As in the case of the Exradin A10 chamber, this discrepancy could arise from the difference between detailed and mixed simulation—which, as mentioned above, is more notorious for small volume ionization chambers like the IBA PPC-05.

3.2. Proton beam qualities

Table 5 shows the Monte Carlo calculated beam quality correction factors in monoenergetic proton beams for all the ionization chambers studied in this work, at a reference depth of $2\,\mathrm{g\,cm^{-2}}$, as a function of the initial energy of the beam. The uncertainty estimate shown is the combined standard uncertainty of f_Q (type A), f_{Q_0} (type A) and $W_{\mathrm{air},Q}/W_{\mathrm{air},Q_0}$ (type B). Note that f_Q factors may be obtained by simply dividing the k_Q factors in table 5 by the corresponding W_{air} ratio and f_{Q_0} factor in table 3, or table 4.

Table 5 shows that the adoption of new I-values results in an average increase in k_Q of about 0.3%—changes in k_Q factors are, however, strongly dependent on the ionization chamber model. For plane-parallel chambers changes in k_Q range from −0.6% up to 1.6%; for cylindrical chambers they range from −0.1% to 1%. For the NE 2571 we

Table 5: Monte Carlo calculated k_Q factors for monoenergetic proton beams, at the reference depth of $2\,\mathrm{g\,cm^{-2}}$, as a function of the initial proton energy. The values within parenthesis correspond to one standard uncertainty in the last digit.

$I_w = 75\,\mathrm{eV}$; $I_g = 78\,\mathrm{eV}$; $W_{air,Q}/W_{air,Q_0} = 1.008$

Ionization	E (MeV)				
chamber	70	100	150	200	250
Exradin					
A10	1.012(6)	1.019(6)	1.007(6)	1.020(6)	1.013(6)
A11	1.012(6)	1.023(5)	1.022(5)	1.025(5)	1.022(6)
A11TW	1.031(6)	1.030(5)	1.030(5)	1.032(5)	1.029(6)
IBA					
NACP-02	0.983(5)	0.988(5)	0.987(5)	0.986(5)	0.990(5)
PPC-05	0.994(5)	1.003(5)	0.999(5)	1.001(5)	1.004(6)
PPC-40	0.991(5)	0.991(5)	0.992(5)	0.993(5)	0.991(5)
PTW					
Adv. Markus	1.007(6)	1.002(6)	0.991(6)	1.000(7)	0.995(7)
Markus	1.004(6)	1.006(6)	1.000(6)	0.999(6)	0.992(6)
Roos	0.992(5)	0.993(5)	0.993(5)	0.995(5)	0.994(5)
IBA					
FC65-G	1.065(5)	1.036(5)	1.022(5)	1.021(5)	1.021(5)
FC65-P	1.066(5)	1.037(5)	1.022(5)	1.022(5)	1.019(5)
NE					
2571	1.064(5)	1.037(5)	1.022(5)	1.022(5)	1.024(5)

$I_w = 78\,\mathrm{eV}$; $I_g = 81.1\,\mathrm{eV}$; $W_{air,Q}/W_{air,Q_0} = 1.014$

Ionization	E (MeV)				
chamber	70	100	150	200	250
Exradin					
A10	1.013(6)	1.013(6)	1.023(6)	1.021(6)	1.021(6)
A11	1.014(5)	1.026(5)	1.023(5)	1.025(5)	1.028(6)
A11TW	1.034(6)	1.039(5)	1.038(5)	1.034(5)	1.038(6)
IBA					
NACP-02	0.981(5)	0.987(5)	0.987(5)	0.988(5)	0.989(5)
PPC-05	0.990(5)	1.003(5)	1.007(5)	1.003(5)	1.004(6)
PPC-40	0.992(5)	0.996(5)	0.998(5)	0.996(5)	0.997(5)
PTW					
Adv. Markus	1.001(6)	0.997(6)	1.003(6)	1.002(7)	1.006(7)
Markus	1.002(6)	1.002(6)	1.012(6)	1.008(6)	1.007(6)
Roos	0.993(5)	0.994(5)	0.998(5)	0.999(5)	0.999(5)
IBA					
FC65-G	1.067(5)	1.040(5)	1.031(5)	1.025(5)	1.020(5)
FC65-P	1.065(5)	1.039(5)	1.029(5)	1.025(5)	1.022(5)
NE					
2571	1.069(5)	1.043(5)	1.032(5)	1.027(5)	1.023(5)

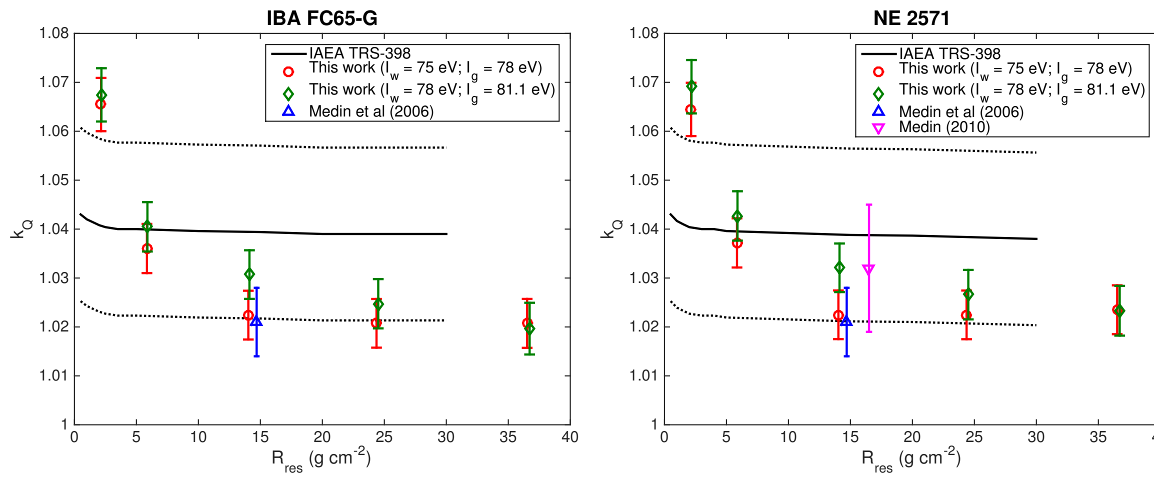

(a) (b)

Figure 1: Comparison of the Monte Carlo k_Q factors for cylindrical ionization chambers calculated in this work and IAEA TRS-398 k_Q factors (——), calculated using ICRU I-values, as a function of R_{res}. The uncertainty bars and dashed lines (- - - -) correspond to one standard uncertainty in the data points and IAEA TRS-398 values, respectively.

obtained an average increase in k_Q of about 0.5%, which agrees within one standard uncertainty with the estimate of Andreo *et al* (2013) of no changes (based on the assumption of negligible perturbation effects).

Figure 1 and figure 2 show a comparison between the k_Q factors of some of the ionization chambers studied in this work (calculated with the two sets of I-values) and the k_Q factors tabulated in IAEA TRS-398 (calculated with ICRU I-values), as a function of the residual range—see table 1 for energy-range equivalence. Figure 1 shows the k_Q factors for cylindrical ionization chambers and it includes the experimental values of Medin *et al* (2006) and Medin (2010), determined with water calorimetry. Figure 2 shows the k_Q factors for plane-parallel chambers.

All the k_Q factors calculated in this work using ICRU I-values agree within 2.3% or better with the k_Q factors tabulated in IAEA TRS-398 and within 1% or better with the experimental values of Medin *et al* (2006) and Medin (2010). The k_Q factors calculated using $I_{\text{w}} = 78\,\text{eV}$ and $I_{\text{g}} = 81.1\,\text{eV}$ also agree within 1.1% or better with the experimental values. Despite this agreement, the dependence of our k_Q factors with the residual range shows a different trend than IAEA TRS-398 values. Figure 1 shows that for cylindrical chambers the variation of our k_Q factors with the residual range is of the order of 5% (within a R_{res} range from 2 to 37 g cm^{-2}), much larger than that of IAEA TRS-398 values (smaller than 0.5%). Such a variation is mainly due to the increase of our k_Q factors at small residual ranges, which in turn is due to the fact that the reference point of the chamber—and not its effective point of measurement—is positioned at the reference measurement depth (Gomà *et al* 2014, Gomà *et al* 2015).

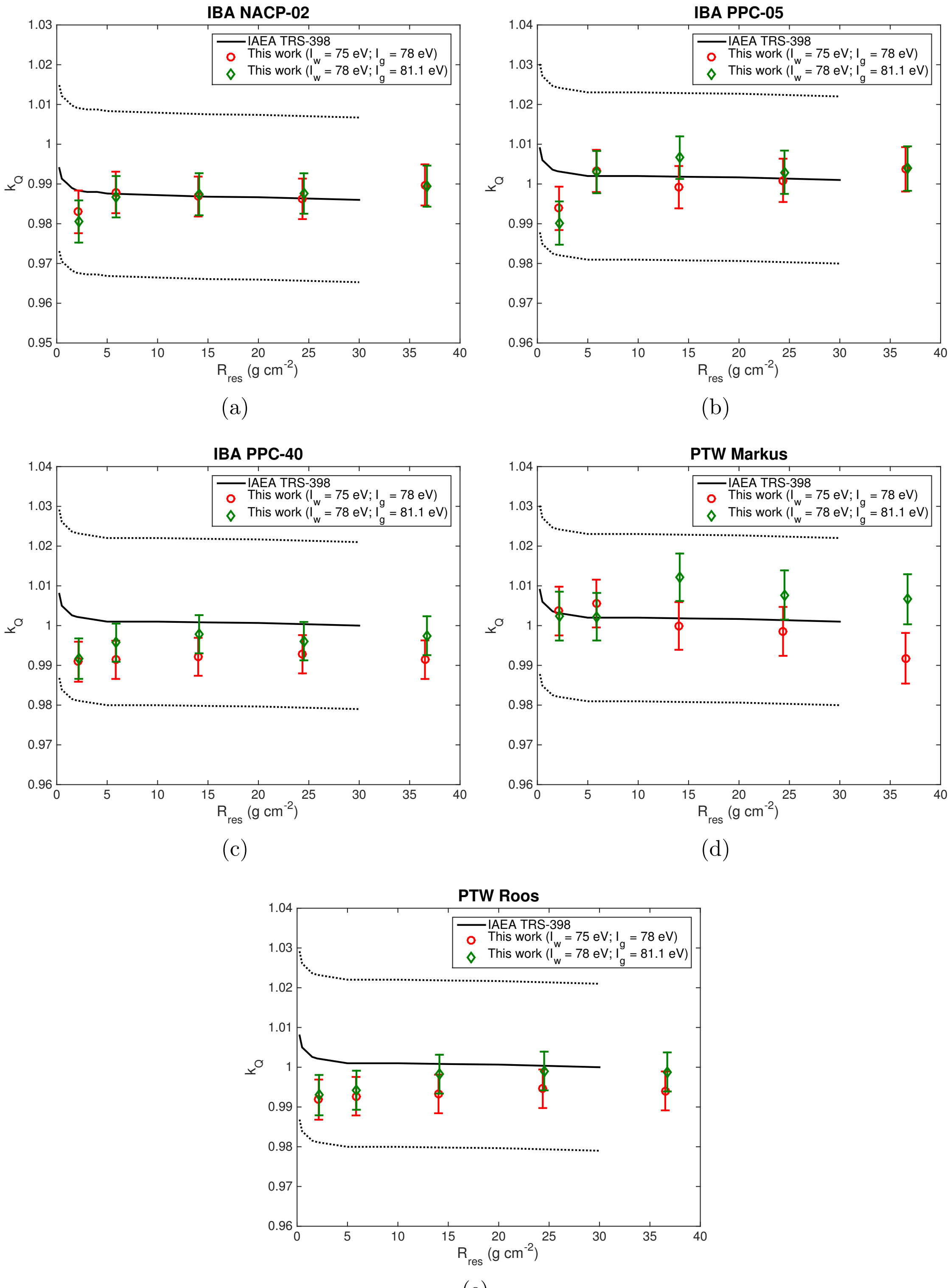

Figure 2: Comparison of the Monte Carlo k_Q factors for plane-parallel ionization chambers calculated in this work and IAEA TRS-398 k_Q factors (——), calculated using ICRU I-values, as a function of R_{res}. The uncertainty bars and dashed lines (- - - -) correspond to one standard uncertainty in the data points and IAEA TRS-398 values, respectively.

Table 6: Ratio of k_Q factors in a 70 MeV monoenergetic proton beam, at the reference depth of $2\,\mathrm{g\,cm^{-2}}$, for different ionization chambers studied in this work and comparison with experimental values in the literature for non-modulated beams. The values within parenthesis correspond to one standard uncertainty in the last digit.

Ionization chambers	This work $I_\mathrm{w}=75\,\mathrm{eV}$ $I_\mathrm{g}=78\,\mathrm{eV}$	$I_\mathrm{w}=78\,\mathrm{eV}$ $I_\mathrm{g}=81.1\,\mathrm{eV}$	Palmans *et al* (2001)	Palmans *et al* (2002)
IBA FC65-G/NE 2571	1.001(2)	0.998(2)	0.997(2)	
IBA NACP-02/NE 2571	0.923(3)	0.917(3)		0.930(3)
PTW Markus/NE 2571	0.943(4)	0.938(4)		0.940(3)
PTW Roos/NE 2571	0.932(2)	0.929(2)		0.937(3)
R_res ($\mathrm{g\,cm^{-2}}$)	2.15	2.18	2.65	2.65

Figure 2 shows that for plane-parallel ionization chambers the agreement between our k_Q factors and IAEA TRS-398 values is better (almost always within 1%) than for cylindrical ionization chambers. However, the variation of the k_Q factors with the residual range seems to follow a different trend. Whereas IAEA TRS-398 k_Q factors decrease slightly with increasing residual range, our k_Q factors seem to slightly increase with increasing residual range. This might be simply a consequence of not assuming a constant $p_Q=1$.

Excluding the case of cylindrical chambers at small residual ranges (because of the reasons mentioned above), all our k_Q factors calculated using ICRU I-values agree with the IAEA TRS-398 values within the standard uncertainty stated in the Code of Practice. Compatible with this agreement is the fact that our mean k_Q values and IAEA TRS-398 mean values may differ by up to 1.8% for some ionization chamber models. Furthermore, these differences (between mean k_Q values) are strongly dependent on the ionization chamber model and the proton beam quality. Such a dependence seems to indicate that perturbation correction factors in proton beams could be significantly different from unity, at least for the some of the ionization chambers studied in this work. For graphite-walled Farmer chambers, for instance, we found that for $R_\mathrm{res} > 14\,\mathrm{g\,cm^{-2}}$ the differences between our mean k_Q values and IAEA TRS-398 values are of about 1.7%. Part of these differences (0.8–0.9%) arise from a higher f_{Q_0} factor ($f_{Q_0}=1.111$–1.112) than that in IAEA TRS-398 ($f_{Q_0}=1.102$). The remaining part arises from a smaller f_Q factor, pointing at $p_Q \sim 0.992(2)$, slighly lower than the value calculated by Palmans (2011) ($p_Q=0.9965$).

To further validate the Monte Carlo k_Q factors calculated in this work, table 6 and table 7 compare the ratio of k_Q factors (k_Q/k_Q^ref) for some of the ionization chambers studied in this work with experimental data published in the literature. Note that k_Q ratios of two ionization chambers have the advantage that they do not depend on the adoption of specific W_air values. Palmans *et al* (2001) and Palmans *et al* (2002)

Table 7: Ratio of k_Q factors in a 100 MeV monoenergetic proton beam, at the reference depth of $2\,\mathrm{g\,cm^{-2}}$, for different ionization chambers studied in this work and comparison with experimental values in the literature for non-modulated beams. The values within parenthesis correspond to one standard uncertainty in the last digit.

Ionization chamber	This work $I_\mathrm{w}=75\,\mathrm{eV}$ $I_\mathrm{g}=78\,\mathrm{eV}$	$I_\mathrm{w}=78\,\mathrm{eV}$ $I_\mathrm{g}=81.1\,\mathrm{eV}$	Gomà *et al* (2015)
IBA NACP-02/IBA FC65-G	0.954(3)	0.948(3)	0.943(4)
PTW Adv. Markus/IBA FC65-G	0.967(5)	0.958(5)	0.949(4)
PTW Markus/IBA FC65-G	0.971(4)	0.963(4)	0.953(4)
PTW Roos/IBA FC65-G	0.958(2)	0.955(2)	0.960(4)
R_res ($\mathrm{g\,cm^{-2}}$)	5.85	5.89	5.93

determined experimentally the ratio of k_Q factors between different ionization chambers and the NE 2571 chamber (as reference chamber) for a non-modulated proton beam of $R_\mathrm{res}=2.65\,\mathrm{cm}$. In their work the authors reported p_Q ratios, instead of k_Q ratios, after applying a serie of theoretical corrections to the experimental data. Herein we reverted these corrections, so that table 6 shows the experimental k_Q ratios obtained by Palmans *et al* (2001) and Palmans *et al* (2002). Also Gomà *et al* (2015) determined the ratio of k_Q factors for different ionization chambers in a proton beam of $R_\mathrm{res}\simeq 6\,\mathrm{cm}$. The values shown in table 7 correspond to the results reported for a non-modulated proton beam. The k_Q ratios calculated in this work using ICRU I-values were found to agree within 0.4%, 0.7% and 1.9%, or better, with the experimental values of Palmans *et al* (2001), Palmans *et al* (2002) and Gomà *et al* (2015), respectively. The k_Q ratios calculated using $I_\mathrm{w}=78\,\mathrm{eV}$ and $I_\mathrm{g}=81.1\,\mathrm{eV}$ were found to agree within 0.1%, 1.3% and 1.0%, or better, with the experimental values of Palmans *et al* (2001), Palmans *et al* (2002) and Gomà *et al* (2015), respectively.

It is worth mentioning again that the k_Q factors calculated in this work are based on the assumption that the contribution to the absorbed dose to water at the reference depth from secondary protons and heavier charged particles generated in the vicinity of z_ref is comparable to the contribution to the absorbed dose to air in the ionization chamber sensitive volume from secondary protons and heavier charged particles generated in the ionization chamber materials. This assumption might affect different ionization chambers differently, depending on the materials they are made of. Nevertheless, and despite this assumption, we found good agreement between our Monte Carlo calculated k_Q factors and the experimental data published in the literature.

Finally, it is important to point out that the k_Q factors calculated in this work include inherently a correction for dose gradient effects in monoenergetic proton beams. Therefore, they should not be used in modulated proton beams, where dose gradients are much smaller.

4. Conclusions

This work calculated f_{Q_0} factors (in ^{60}Co gamma radiation) and k_Q factors in monoenergetic proton beams for a wide range of ionization chambers using Monte Carlo simulation. We used the electronic stopping powers resulting from the adoption of two different sets of I-values for water and graphite: ICRU 37 and ICRU 49 I-values ($I_{\rm w} = 75\,{\rm eV}$; $I_{\rm g} = 78\,{\rm eV}$) and new I-values proposed by Andreo *et al* (2013) and Burns *et al* (2014) ($I_{\rm w} = 78\,{\rm eV}$; $I_{\rm g} = 81.1\,{\rm eV}$). The f_{Q_0} factors calculated in this work were in good agreement with other Monte Carlo calculated values published in the literature. Except for the case of cylindrical chambers at small residual ranges, our Monte Carlo calculated k_Q factors agreed with the values tabulated in IAEA TRS-398 and the experimental values in the literature within their stated standard uncertainties. The results of this work point at perturbation correction factors in proton beams that may differ significantly from unity for some of the ionization chambers studied. Nevertheless, it is believed that an independent calculation of k_Q factors in proton beams—by other authors and, ideally, with a different Monte Carlo code—would be of interest for the scientific community in order to validate, or question, the k_Q factors reported in this work.

Acknowledgments

The authors would like to thank David Burns for providing the spectrum of the BIPM ^{60}Co-source in a numerical form. CG would also like to thank Jan Würfel and Frank Schwamm (PTW-Freiburg) and Brian Hooten (Standard Imaging) for providing the descriptions of the geometry and material composition of several ionization chambers. The authors are also thankful to Bryan Muir, Llorenç Brualla and Antonio Lallena for sharing their f_{Q_0}-factor results and for giving us permission to include them in this work. Especial thanks go to Francesc Salvat for providing the Monte Carlo simulation package PENH. JS thanks financial support from the Spanish Ministerio de Economía y Competitividad (Project No. FIS2012-38480), from the Generalitat de Catalunya (Project No. 2014 SGR 846) and from the Spanish Networking Research Center CIBER-BBN.

References

Agostinelli S *et al* 2003 GEANT4—a simulation toolkit *Nucl. Instrum. Methods Phys. Res. A* **506** 250–303

Aird E G A and Farmer F T 1972 The design of a thimble chamber for the Farmer dosemeter *Phys. Med. Biol.* **17** 169–74

Andreo P 1992 Absorbed dose beam quality factors for the dosimetry of high-energy photon beams *Phys. Med. Biol.* **37** 2189–211

Andreo P, Burns D T, Hohlfeld K, Huq M S, Kanai T, Laitano F, Smyth V and Vynckier S 2000 Absorbed dose determination in external beam radiotherapy: an International Code of Practice for dosimetry based on standards of absorbed dose to water *IAEA Technical Report Series No. 398* (Vienna: IAEA)

Andreo P, Wulff J, Burns D T and Palmans H 2013 Consistency in reference radiotherapy dosimetry: resolution of an apparent conundrum when ^{60}Co is the reference quality for charged-particle and photon beams *Phys. Med. Biol.* **58** 6593–621

Arce P *et al* 2014 GAMOS: a framework to do GEANT4 simulations in different physics fields with an user-friendly interface *Nucl. Instrum. Methods A* **735** 304–13

Baró J, Sempau J, Fernández-Varea J M and Salvat F 1995 PENELOPE: an algorithm for Monte Carlo simulation of the penetration and energy loss of electrons and positrons in matter *Nucl. Instrum. Methods B* **100** 31–46

Battistoni G, Muraro S, Sala P R, Cerutti F, Ferrari A, Roesler S, Fassò A and Ranft J 2007 The FLUKA code: description and benchmarking *AIP Conf. Proc.* **896** 31–49

Berger M J 1963 Monte Carlo calculation of the penetration and diffusion of fast charged particles *Methods in Computational Physics* ed Alder B, Fernbach S and Rotenberg M (New York: Academic Press) pp 135–215

Burns D T 2003 Calculation of $k_{\rm wall}$ for ^{60}Co air-kerma standards using PENELOPE *CCRI(I)/03-40*

Burns D T, Picard S, Kessler C and Roger P 2014 Use of the BIPM calorimetric and ionometric standards in megavoltage photon beams to determine $W_{\rm air}$ and $I_{\rm c}$ *Phys. Med. Biol.* **59** 1353–65

Cirrone G A P *et al* 2009 Hadrontherapy: an open source, GEANT4-based application for proton-ion therapy studies *IEEE Nuclear Science Symp. Conf. Record* pp 4186–9

Elles S, Ivanchenko V N, Maire M and Urban L 2008 GEANT4 and Fano cavity test: where are we? *Journal of Physics: Conference Series* **102** 012009

Erazo F, Brualla L and Lallena A M 2014 Electron beam quality k_{Q,Q_0} factors for various ionization chambers: a Monte Carlo investigation with PENELOPE *Phys. Med. Biol.* **59** 6673–91

Erazo F and Lallena A M 2013 Calculation of beam quality correction factors for various thimble ionization chambers using the Monte Carlo code PENELOPE *Physica Medica* **29** 163–70

Ferrari A, Sala P R, Fassò A and Ranft J 2005 FLUKA: a multi-particle transport code *CERN-2005-010, INFN TC_05/11 , SLAC-R-773*

Fippel M and Soukup M 2004 A Monte Carlo dose calculation algorithm for proton therapy *Med. Phys.* **31** 2263–73

Gomà C, Andreo P and Sempau J 2013 Spencer–Attix water/medium stopping-power ratios for the dosimetry of proton pencil beams *Phys. Med. Biol.* **58** 2509–22

Gomà C, Lorentini S, Meer D and Safai S 2014 Proton beam monitor chamber calibration *Phys. Med. Biol.* **59** 4961–71

Gomà C, Hofstetter-Boillat B, Safai S and Vörös S 2015 Experimental validation of beam quality correction factors for proton beams *Phys. Med. Biol.* **60** 3207–16

González-Castaño D M, Hartmann G H, Sánchez-Doblado F, Gómez F, Kapsch R-P, Pena J and Capote R 2009 The determination of beam quality correction factors: Monte Carlo simulations and measurements *Phys. Med. Biol.* **54** 4723–41

ICRU International Commission on Radiation Units and Measurements 1984 Stopping powers for electrons and positrons *ICRU Report No. 37* (Bethesda, MD: International Commission on Radiation Units and Measurements)

ICRU International Commission on Radiation Units and Measurements 1993 Stopping powers and ranges for protons and alpha particles *ICRU Report No. 49* (Bethesda, MD: International Commission on Radiation Units and Measurements)

ICRU International Commission on Radiation Units and Measurements 2007 Prescribing, recording and reporting proton beam therapy *ICRU Report No. 78* (Bethesda, MD: International Commission on Radiation Units and Measurements)

JCGM Joint Commitee for Guides in Metrology 2008 Evaluation of measurement data — Guide to the expression of uncertainty in measurement *JCGM 100:2008*

Kawrakow I 2000a Acurate condensed history Monte Carlo simulation of electron transport. I. EGSnrc, the new EGS4 version *Med. Phys.* **27** 485–98

Kawrakow I 2000b Accurate condensed history Monte Carlo simulation of electron transport. II. Application to ion chamber response simulations *Med. Phys.* **27** 499–513

Klingebiel M, Kunz M, Colbus S, Zink K and Wulff J 2011 Testing the accuracy of electron transport in the Monte Carlo code FLUKA for calculation of ionization chamber wall perturbation factors *Proc. Int. Symp. on Standards, Applications and Quality Assurance in Medical Radiation Dosimetry (Vienna, 2010)* (Vienna: IAEA) pp 319–29

Medin J 2010 Implementation of water calorimetry in a 180 MeV scanned pulsed proton beam including an experimental determination of k_Q for a Farmer chamber *Phys. Med. Biol.* **55** 3287–98

Medin J and Andreo P 1997 Monte Carlo calculated stopping-power ratios, water/air, for clinical proton dosimetry (50-250 MeV) *Phys. Med. Biol.* **42** 89–105

Medin J, Ross C K, Klassen N V, Palmans H, Grusell E and Grindborg J 2006 Experimental determination of beam quality factors, k_Q, for two types of Farmer chamber in a 10 MV photon and a 175 MeV proton beam *Phys. Med. Biol.* **51** 1503–21

Muir B R, McEwen M R and Rogers D W O 2012 Beam quality conversion factors for parallel-plate ionization chambers in MV photon beams *Med. Phys.* **39** 1618–31

Muir B R and Rogers D W O 2010 Monte Carlo calculations of k_Q, the beam quality conversion factor *Med. Phys.* **37** 5939–50

Muir B R and Rogers D W O 2014 Monte Carlo calculations of electron beam quality conversion factors for several ion chamber types *Med. Phys.* **41** 111701

NE Nuclear Enterprises 1984 Radiological Application Report No. 3 Issue 3

Paganetti H 2002 Nuclear interactions in proton therapy: dose and relative biological effect distributions originating from primary and secondary particles *Phys. Med. Biol.* 747–64

Palmans H 2006 Perturbation factors for cylindrical ionization chambers in proton beams. Part I: corrections for gradients *Phys. Med. Biol.* **51** 3483–501

Palmans H 2011 Secondary electron perturbations in Farmer type ion chambers for clinical proton beams *Proc. Int. Symp. on Standards, Applications and Quality Assurance in Medical Radiation Dosimetry (Vienna, 2010)* (Vienna: IAEA) pp 309–17

Palmans H and Verhaegen F 1998 Monte Carlo study of fluence perturbation effects on cavity dose response in clinical proton beams *Phys. Med. Biol.* **43** 65–89

Palmans H, Verhaegen F, Denis JM, Vynckier S and Thierens H 2001 Experimental $p_{\rm wall}$ and $p_{\rm cel}$ correction factors for ionization chambers in low-energy clinical proton beams *Phys. Med. Biol.* **46** 1187–204

Palmans H, Verhaegen F, Denis JM and Vynckier S 2002 Dosimetry using plane-parallel ionization chambers in a 75 MeV clinical proton beam *Phys. Med. Biol.* **47** 2895–905

Panettieri V, Sempau J and Andreo P 2008 Chamber-quality factors in ^{60}Co for three plane-parallel chambers for the dosimetry of electrons, protons and heavier charged particles: PENELOPE Monte Carlo simulations *Phys. Med. Biol.* **53** 5917–26

Poon E, Seuntjens J and Verhaegen F 2005 Consistency test of the electron transport algorithm in the GEANT4 Monte Carlo code *Phys. Med. Biol.* 681–694

Salvat F 2013 A generic algorithm for Monte Carlo simulation of proton transport *Nucl. Instrum. Methods B* **136** 144–59

Salvat F 2014 PENELOPE 2014: A code system for Monte Carlo simulation of electron and photon transport (Issy-les-Moulineaux: OECD Nuclear Energy Agency).

Sempau J, Acosta E, Baró J, Fernández-Varea J M and Salvat F 1997 An algorithm for Monte Carlo simulation of coupled electron-photon transport *Nucl. Instrum. Methods B* **132** 377–90

Sempau J, Andreo P, Aldana J, Mazurier J and Salvat F 2004 Electron beam quality correction factors for plane-parallel ionization chambers: Monte Carlo calculations using the PENELOPE system *Phys. Med. Biol.* **49** 4427–44

Sempau J and Andreo P 2006 Configuration of the electron transport algorithm of PENELOPE to simulate ion chambers *Phys. Med. Biol.* **51** 3533–48

Sempau J, Badal A and Brualla L 2011 A PENELOPE-based system for the automated Monte Carlo simulation of clinacs and voxelized geometries—application to far-from-axis fields *Med. Phys.* **38** 5887–95

Seuntjens J, Kawrakow I, Borg J, Hobeila F and Rogers D W O 2002 Calculated and measured air-kerma response of ionization chambers in low and medium energy photon beams *Proc. Recent Developments in Accurate Radiation Dosimetry* (Madison, WI: Medical Physics Publishing) pp 69–84

Sterpin E, Sorriaux J and Vynckier S 2013 Extension of PENELOPE to protons: Simulation of nuclear reactions and benchmark with GEANT4 *Med. Phys.* **40** 111705

Vatnitsky S M, Siebers J V and Miller D W 1996 k_Q factors for ionization chamber dosimetry in clinical proton beams *Med. Phys.* **23** 25–31

Verhaegen F and Palmans H 2001 A systematic Monte Carlo study of secondary electron fluence perturbation in clinical proton beams 70–250 MeV for cylindrical and spherical ion chamber *Med. Phys.* **28** 2088–95

Waters L S 2002 MCNPX user's manual *Technical Report LA-UR-02-2607*

Wulff J, Heverhagen J T and Zink K 2008 Monte-Carlo-based perturbation and beam quality correction factors for thimble ionization chambers in high-energy photon beams *Phys. Med. Biol.* **53** 2823–36

Zink K and Wulff J 2008 Monte Carlo calculations of beam quality correction factors k_Q for electron dosimetry with a parallel-plate Roos chamber *Phys. Med. Biol.* **53** 1595–607

Zink K and Wulff J 2012 Beam quality corrections for parallel-plate ion chambers in electron reference dosimetry *Phys. Med. Biol.* **57** 1831–54